K. Karthick\*, S. Malarvizhi, V. Balasubramanian, S.A. Krishnan, G. Sasikala and Shaju K. Albert

# Tensile properties of shielded metal arc welded dissimilar joints of nuclear grade ferritic steel and austenitic stainless steel

DOI 10.1515/jmbm-2017-0005

Abstract: In nuclear power plants, modified 9Cr-1Mo ferritic steel (Grade 91 or P91) is used for constructing steam generators (SG's) whereas austenitic stainless steel (AISI 316LN) is a major structural member for intermediate heat exchanger (IHX). Therefore, a dissimilar joint between these materials is unavoidable. In this investigation, dissimilar joints were fabricated by Shielded Metal Arc Welding (SMAW) process with Inconel 82/182 filler metals. Transverse tensile properties and Charpy V-notch impact toughness for different regions of dissimilar joints of modified 9Cr-1Mo ferritic steel and AISI 316LN austenitic stainless steel were evaluated as per the standards. Microhardness distribution across the dissimilar joint was recorded. Microstructural features of different regions were characterized by optical and scanning electron microscopy. The transverse tensile properties of the joint is found to be inferior to base metals. Impact toughness values of different regions of dissimilar metal weld joint (DMWJ) is slightly higher than the prescribed value. Formation of a soft zone at the outer edge of the HAZ will reduce the tensile properties of DMWJ. The complex microstructure developed at the interfaces of DMWJ will reduce the impact toughness values.

**Keywords:** austenitic stainless steel; dissimilar joint; ferritic steel; impact toughness; shielded metal arc welding; tensile properties.

#### 1 Introduction

Modified 9Cr-1Mo (9Cr-1Mo-VNbN) ferritic steel (grade 91) is widely used in nuclear and fossil-fired power plants due to its high temperature strength and resistance to stress corrosion cracking (SCC). This steel has tempered martensite structure and derives its high temperature strength from the phase transformation induced dislocation sub-structure and interface, inter- and intra-granular precipitation of (V,Nb)(C,N) and chromium rich M<sub>23</sub>C<sub>6</sub> carbides, respectively [1]. Type 316LN (0.02-0.03% C and 0.06-0.08% N) austenitic stainless steel is a major structural material for nuclear power plant components such as reactor vessel, intermediate heat exchanger, and primary sodium systems. This steel has excellent creep and tensile strength over modified 9Cr-1Mo ferritic steel. Nitrogen is added to this steel to enhance the intergranular stress corrosion cracking resistance (IGSCC) [2]. Therefore, a dissimilar joint between ferritic steel and austenitic stainless steel is inevitable.

The operating experience of direct bimetallic (without buttering layer) ferritic/austenitic junction revealed poor performance in power plants. The use of direct bimetallic joint between ferritic steel and austenitic stainless steel has led to several problems in service like thermally induced cyclic stresses resulting from the difference in coefficients of thermal expansion between the ferritic and austenitic steels (difference in coefficient of thermal expansion of these two materials is ~30-40%) [3]. Earlier, ER 308L and 309L were used to join these materials but resulted in premature failures due to carbon migration (formation of the soft zone between modified 9Cr-1Mo and ER308/309) and sigma phase formation. Nickel based consumables (Inconel 82 and Inconel 182) offers the best compromise between these materials because it significantly retards carbon migration and gives improved thermal stability over ER 308L/309L [4].

Cross weld tensile test is most widely used to qualify the weld joint and this test will reveal the weakest region among the weld joint. During the cross weld tensile test, crack initiation will start at the weakest region and

<sup>\*</sup>Corresponding author: K. Karthick, Research Scholar, Centre for Materials Joining and Research (CEMAJOR), Department of Manufacturing Engineering, Annamalai University, Annamalai Nagar – 608 002, Tamil Nadu, India, Tel.: 9488465517, e-mail: karthick.kuppan@gmail.com

**S. Malarvizhi and V. Balasubramanian:** Centre for Materials Joining and Research (CEMAJOR), Department of Manufacturing Engineering, Annamalai University, Annamalai Nagar – 608 002, Tamil Nadu, India

**S.A.** Krishnan: Homi Bhabha National Institute, Indira Gandhi Centre for Atomic Research (IGCAR), Kalpakkam – 603 102, Tamil Nadu, India

**G. Sasikala and Shaju K. Albert:** Indira Gandhi Centre for Atomic Research (IGCAR), Kalpakkam – 603 102, Tamil Nadu, India

failure occurs [5]. Sireesha et al. [6] studied the effect of accelerated thermal cycling on a joint between modified 9Cr-1Mo and alloy 800 with Inconel 82/182 filler. From the study, they found that no cracking and oxide notches were present in the welds even after prolonged thermal cycling [6]. Sireesha et al. [7] investigated the influence of high temperature exposure on mechanical and metallurgical characteristics of dissimilar joint between modified 9Cr-1Mo and Alloy 800 and found that the carbon diffusion to the weld metal is less as compared to 2.25Cr-1Mo and some intermetallic precipitation occurs when the weld metals is aged about 2000 h but the weld metal toughness is adequate as per the PFBR specifications [7]. Lee et al. [8] studied the creep-fatigue damage for a dissimilar metal welds between modified 9Cr-1Mo and 316L stainless steel. From this, no significant damage was observed for both bimetallic (modified 9Cr-1Mo/Inconel 82/316L) and trimetallic configurations (modified 9Cr-Mo/Inconel 82/Alloy 800H/316L) except for filler metals [8].

Rathod et al. [9] investigated mechanical properties of dissimilar joints between SA508 ferritic steel and SS304L stainless steel with Inconel 82/182 consumables and found that the transverse tensile properties of the welds are lower than the respective base metals due to the fine slag inclusions present in the weld metal [9]. Falat et al. [10] analyzed the effects of post weld heat treatment and isothermal aging on T92 steel heat-affected zone mechanical properties of T92/TP316H dissimilar weldments. From this, they found that two step post weld heat treatment will lower the strength and improves the toughness of the joint [10]. Rathod et al. [11] studied mechanical properties variations and comparative evaluation of welding

consumables between SA508 ferritic steel and SS304L stainless steel. From his study, he found that Inconel 82/182 is offered better strength properties over Inconel 52/152 [11]. From the available literature, it was found that there is no papers are reported so far on evaluating the cross weld tensile properties of the dissimilar joint between modified 9Cr-1Mo and SS316LN with Inconel 82/182 filler metals. Hence, the present investigation is focused on the evaluation of cross weld tensile properties and microstructural characteristics of shielded metal arc welded (SMAW) dissimilar joints of nuclear grade ferritic steel and austenitic stainless steel.

# 2 Experimental work

## 2.1 Materials and welding

The base metals used in this investigation are modified 9Cr-1Mo ferritic steel (supplied in normalizing and tempered condition) and AISI 316LN austenitic stainless steel (supplied in solution annealed condition). The dissimilar joints were fabricated by shielded metal arc welding process (SMAW) using Inconel 82/182 filler metals. The Inconel 82 (ø 1.2 mm) is a gas tungsten arc welding (GTAW) filler wire which is used for root and second passes. For the remaining passes SMA electrodes of Inconel 182 (ø 3.12 mm) were used. Before welding, the electrodes are dried in an oven (250°C for 1 h) as per the manufacturer specifications. The chemical compositions and mechanical properties of base and filler metals are presented in Tables 1 and 2 respectively. K-joint

Table 1: Chemical compositions (in wt%).

Elements in (wt%)	Base metals		Filler metals	
	Ferritic steel	Austenitic stainless steel	Inconel 82	Inconel 182
C	0.10	0.02	0.10 max.	0.04
Ni	0.25	12.55	(Ni + Co) 67.01	70.08
Cr	9.06	17.27	18.0-22.0	16.90
Мо	0.79	2.35	_	-
Si	0.18	0.29	0.50 max.	0.69
Mn	0.38	1.69	2.5-3.5	6.20
Cu	0.04	0.04	0.50 max.	0.01
Nb	0.07	0.02	(Nb + Ta) 2.0 - 3.0	2.09
V	0.20	0.04	_	Ti (0.08)
S	0.01	0.02	0.015 max.	0.01
Р	0.01	0.02	0.030 max.	0.007
Fe	Bal.	Bal.	3.0 max.	3.31
Grade	P91	316LN	ENiCr-3	ENiCrFe-3

Table 2: Mechanical properties of base and filler metals.

	0.2% Offset yield strength (MPa)	Ultimate tensile strength (MPa)	Elongation in 50 mm gauge length (%)
Ferritic steel	590	720	19
Austenitic stainless steel	312	590	44
Inconel 82	325	552	30
Inconel 182	325	552	30

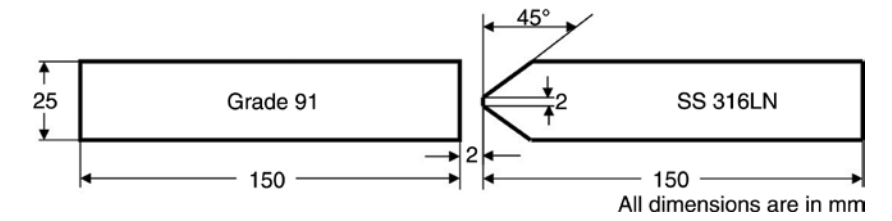


Figure 1: Details of K-joint configuration used in this investigation.

configuration was prepared and the dimension are shown in Figure 1. Before welding the modified 9Cr-1Mo plates were buttered with Inconel 182 electrodes. The preheat temperature of 250°C was maintained throughout the buttering process. After buttering, the plates are subjected to post heating with a temperature of 760°C for 2 h. The post-heating was done in the electrical resistance furnace with a heating rate of 150°C/h and followed by furnace cooling. After post heating buttered modified 9Cr-1Mo plates were subjected to dye penetrant testing (DPT) and free from surface cracks was ensured. The dissimilar joint between buttered modified 9Cr-1Mo and SS 316LN was done in 1G (Flat horizontal) position. The welding parameters used to fabricate the dissimilar metal weld joints (DMWJ) are presented in Table 3. After welding, the DMWJ is subjected to 100% radiography test as per ASME Section V (inspection procedure)

and it was accepted as per ASME Section III (acceptance criteria).

#### 2.2 Mechanical testing and characterization

For mechanical testing, transverse tensile and charpy impact specimens were extracted from the DMWJ. After extraction, the specimens were sliced using wire cut electrical discharge machining (EDM) because the specimens are having a thickness of about 25 mm. Both tensile and impact specimens were prepared as per ASTM E8 and ASTM E23 standards respectively [12, 13]. Tensile tests are carried out at a constant strain rate of 2.8 × 10<sup>-4</sup> s<sup>-1</sup>. Charpy V-notch impact test at room temperature was carried out using accelerated impact tester. The velocity of the pendulum was kept as 5.12 m/s. This velocity is same as normal

Table 3: Welding parameters used to fabricate the DMWJ.

Parameters	Buttering on	Root pass	Remaining
	ferritic steel side	using GTAW	passes by SMAW
Current (A)	80	120	70–85
Voltage (V)	22	18	20-23
Speed (mm/min)	150	100	140-160
Heat input (kJ/mm)	0.56	0.76	0.48-0.59
Electrode diameter (mm)	3.15	2	3.15
Preheat temperature (°C)	250	_	-
Inter-pass temperature (°C)	250	_	-
Post heating (°C)	760/2 h	_	-
Shielding gas flow rate (l/min)	_	Argon 20 l/min	_

Charpy test pendulum velocity as per ASTM E23 standard. Before testing, both tensile and impact specimens were mirror polished in order to ensure the smoothness. The scheme of extraction and the dimensions of the tensile and impact specimens are shown in Figures 2 and 3A and B, respectively.

Microhardness survey across DMWJ was carried out using Vickers microhardness tester. The load and the dwell time was kept at a constant value of 100 g and 15 sec. The distance between two indentations were kept as 0.5 mm for base metal to HAZ and a distance of 0.1 mm was kept for HAZ to fusion interface. Since the joint thickness is about 25 mm, the microhardness survey was carried out along the three lines (top, middle and bottom) and across the cross-section of the DMWI. Microstructural features of DMWJ was carried out using a light optical microscope. The DMWJ was having three different materials, so three different chemical etchants were used to reveal the microstructure. For modified 9Cr-1Mo, Villela's reagent was used. For Inconel 82/182, a solution which contains 5 g FeCl<sub>2</sub>, few drops of HCl and 100 ml H<sub>2</sub>O was used as an etchant. For SS316LN, 10 ml HNO<sub>3</sub>, 20 ml HCl and 30 ml of H<sub>2</sub>O was used. Fracture surfaces of tensile and impact

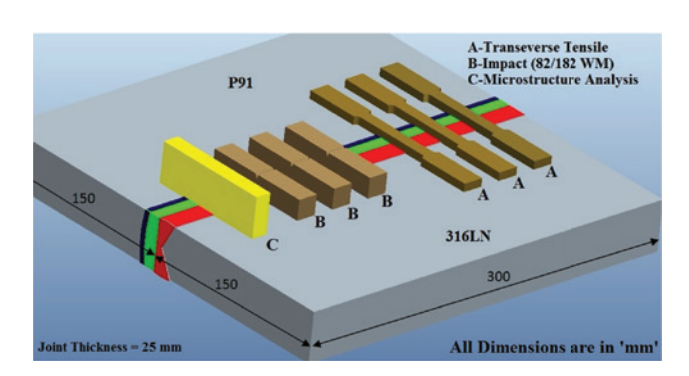


Figure 2: Scheme of extraction of tensile and impact specimens.

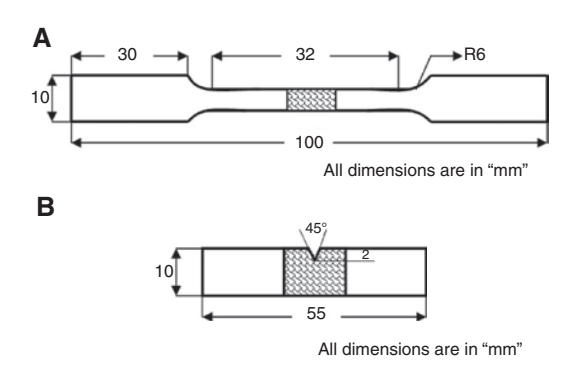


Figure 3: Dimensions of tensile and impact specimens.
(A) Dimensions of the tensile specimen – Unnotch, (B) Dimensions of tensile and impact specimens.

specimens were analyzed using scanning electron microscopy. Before SEM analysis, the fractured surfaces were degreased with acetone.

#### 3 Results and discussion

#### 3.1 Tensile properties

Room temperature tensile test was carried out for base metals and DMWI as per the standards [12]. During tensile test, load-displacement curve was recorded and then it was converted into engineering stress-engineering strain curve. Figure 4 shows the stress-strain plots for base metals and DMWJ. The important data's such as yield strength, ultimate tensile strength, and percentage elongation are presented in Table 4. Three specimens were tested in each case and the average values are presented with standard deviation. All the three transverse tensile specimens were failed in the modified 9Cr-1Mo base metal side. In all the three specimens, the location of fracture is about 3-4.5 mm from the fusion interface of modified 9Cr-1Mo to Inconel 182 buttering. The tensile strength of DMWJ is lower than the base metals which is 39% lower than modified 9Cr-1Mo ferritic steel and 14% lower than SS316LN. Few authors [14, 15] reported that a soft zone was formed at the outer edge of the HAZ and this soft zone consisted of coarsened martensitic substructure with reduced dislocation density due to intercritical heating (between AC, and AC,) during the weld thermal cycle. In this investigation, the transverse tensile specimens were failed at the outer edge of HAZ to base metal interface which may consist of inter-critical HAZ.

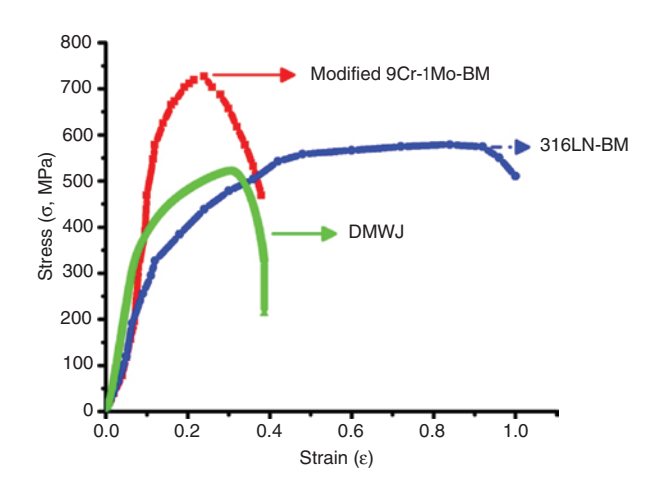


Figure 4: Engineering stress-strain curves.

Table 4: Tensile and impact toughness properties of base metals and DMWJ.

	0.2% Yield strength (MPa)	Ultimate tensile strength (MPa)	Elongation in 25 mm gauge length (%)	Location of failure	Charpy impact toughness @RT (J)
P91-BM	590 (15.09)	720 (6.11)	19 (1)	_	210 (10.5)
SS316LN-BM	312 (18.33)	590 (18.33)	44 (1.52)	-	240 (12)
DMWJ-TTT	394 (8.62)	519 (8.02)	9 (0.57)	P91 BM	116 (5.8)

The values given in the brackets are standard deviations.

## 3.2 Impact toughness

Charpy V-notch impact toughness at room temperature for different regions of DMWJ are presented in Table 4. At each region, three specimens were tested and the average results with standard deviation are presented in the Table 4. Among various regions, HAZ of 316LN yielded highest toughness (146 J) followed by Inconel 82/182 weld metal, Inconel 182 buttering, and HAZ of modified 9Cr-1Mo ferritic steel. The presence of carbon enriched hard zone in the HAZ of the modified 9Cr-1Mo side will lower the impact toughness (96 J) than other regions of DMWJ. This may arise due to carbon migration from the low chromium ferritic steel side to high chromium Inconel 182 buttering [16]. The use of Inconel fillers will not completely eliminate the carbon migration but it will significantly impede compared to chromium rich stainless steel fillers. The energy absorbed in each region is slightly greater than minimum prescribed value of 80 J [17] and this value is for U-notched specimens. In this investigation, Charpy V-notch is used to determine the impact toughness which will have high constraint effect than standard U-notched specimens.

#### 3.3 Fracture surface analysis

The Fracture surfaces for modified 9Cr-1Mo ferritic steel (both tensile and impact) base metal are shown in Figure 5A-B). Fine dimples along with tear ridges was visible in fracture surfaces of tensile specimen (Figure 5A) whereas some flat facets was observed (Figure 5B) in the charpy impact toughness specimen. The impact toughness for modified 9Cr-1Mo ferritic steel is around 210 J. In Figure 5C, large cavities were observed in the fracture surfaces of austenitic stainless steel base metal which shows that large plastic deformation is observed by this steel before failure. The fracture surfaces for impact specimen of austenitic stainless steel is shown in Figure 5D which consists of quasi-cleavage pattern and the crack propagated opposite to the loading direction. The impact toughness for austenitic stainless steel is around 240 J.

The fracture surfaces of tensile and impact toughness specimens of DMWJ is shown in Figure 5E-F. The failure location of the transverse tensile specimen is at the outer edge of HAZ of modified 9Cr-1Mo ferritic steel. Hence the fracture surfaces of DMWI is similar to that of modified 9Cr-1Mo ferritic steel base metal. Fracture surfaces of charpy impact specimen is shown in Figure 5F which consists of fine and deep dimples with tear ridges and the cracks are oriented opposite to the loading direction. The impact toughness for Inconel 82/182 weld metal is found to be inferior than the base metals due to fine slag inclusions associated with the SMAW process. The impact toughness of weld metal is around 114 J which is somewhat higher than the minimum prescribed value of 80 J as per the prototype fast breeder reactor (PFBR) specifications.

#### 3.4 Microhardness survey

Figure 6 shows the microhardness variation across DMWJ. The hardness range for the modified 9Cr-1Mo base metal is 225-240 Hv and 200-240 Hv for SS 316LN. Due to the large thickness of the joint, the hardness was measured at top, middle and bottom (in thickness direction) of the DMWJ and presented in Figure 6 for better understanding. The highest hardness of about 250 Hv is recorded at the interface between modified 9Cr-1Mo to Inconel 182 buttering this may be due to the presence of carbon enriched hard zone formed during carbon migration. The hardness remains same for both buttering and welding. The lowest hardness of about 170-180 Hv is recorded at the outer edge of HAZ which is exactly 4-5 mm from the interface between modified 9Cr-1Mo to Inconel 182 buttering. These results are also consistent with the transverse tensile test (failure occurs at 4-5 mm from the interface). The HAZ of 316LN is having higher hardness compared to its base metal due to repeated tempering caused by multi pass welding. From the hardness survey, a non-uniform hardness profile was observed across the DMWJ and a soft or weakest zone is identified at the outer edge of HAZ.

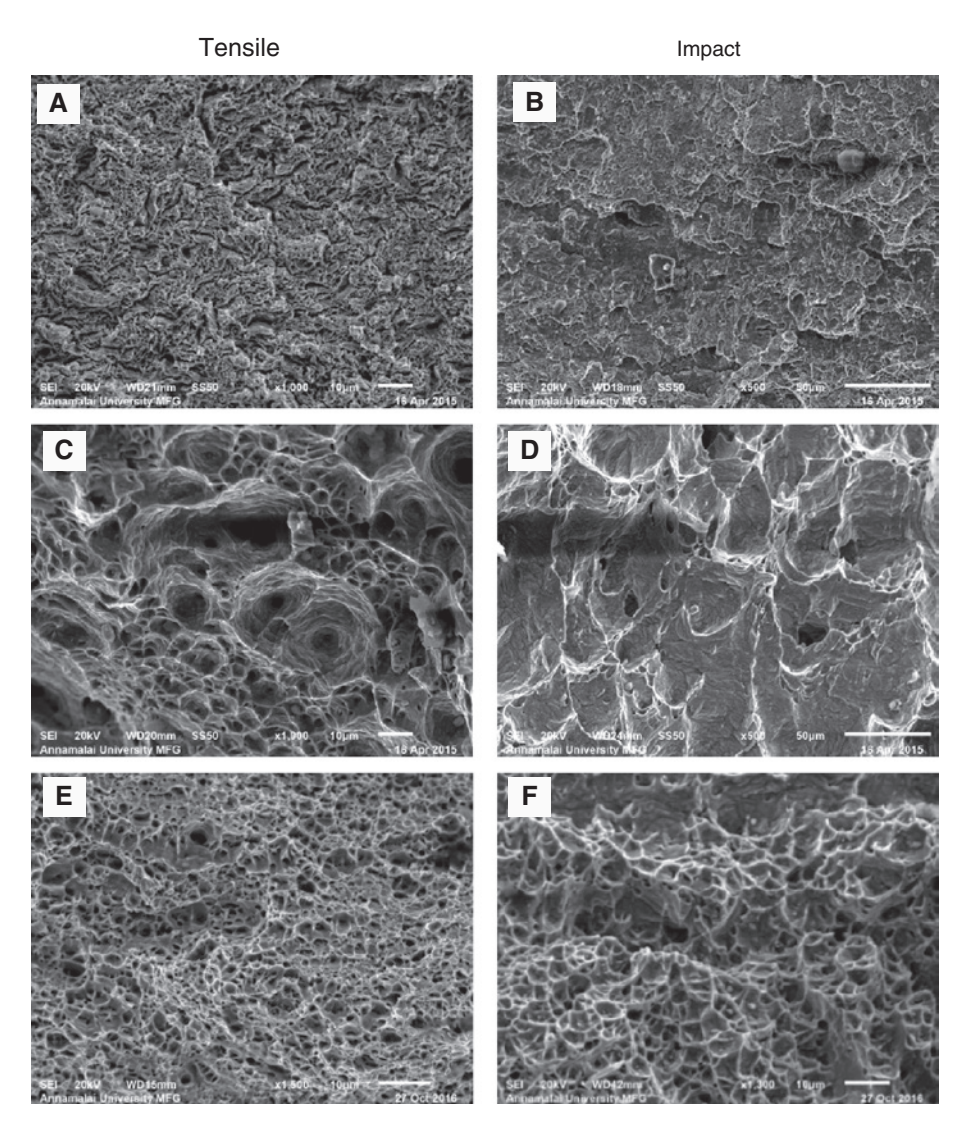


Figure 5: SEM fractographs of tensile and impact specimens.

(A and B) Ferritic steel – BM, (C and D) Austenitic stainless steel – BM, (E and F) DMWJ.

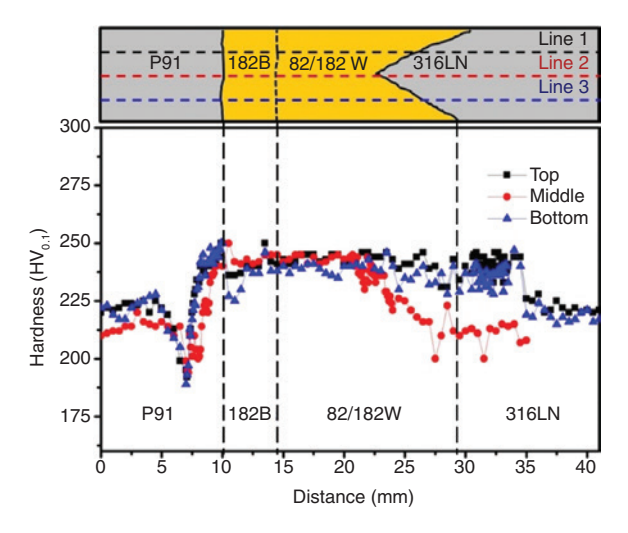


Figure 6: Microhardness variations across DMWJ.

#### 3.5 Microstructural characterization

The microstructure of modified 9Cr-1Mo base metal is shown in Figure 7A. It consists of tempered martensite with prior austenitic grain boundaries and some of the secondary phase particles are finely distributed in grain boundaries and within the grains. These secondary phase particles are presumably of  $M_{23}C_6$  type and some of Nb and V rich (C, N) phases are also presented in the grain boundaries [10]. In addition to that, the martensite structure is having high dislocation density even after tempering treatment (760°C/1 h) which shows the tempering time is not sufficient. The optical micrograph of SS 316LN is shown in Figure 7B which consists of fully equiaxed austenite grains with annealing twins and  $\delta$ -ferrite was presented in the grain boundaries in the form of stringers.

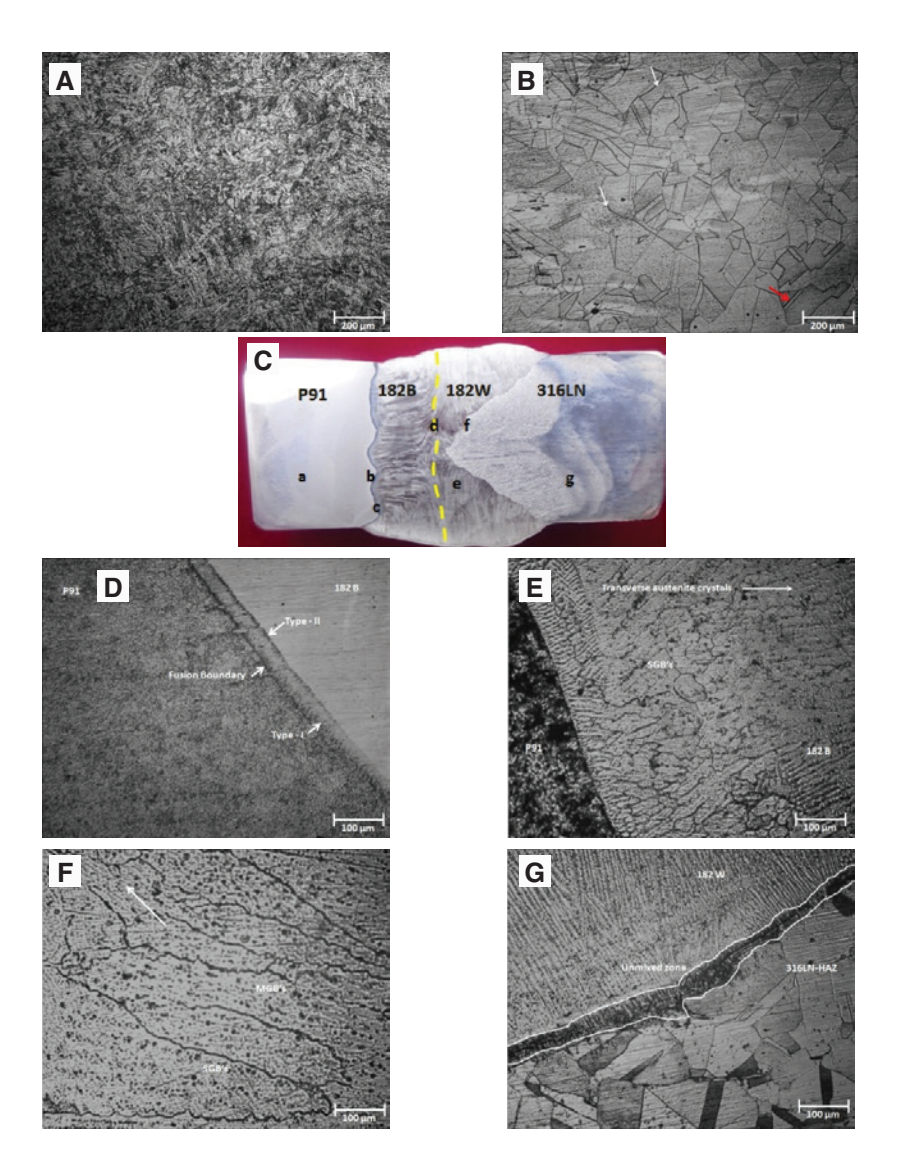


Figure 7: Optical micrographs of base metals and DMWJ. (A) Modified 9Cr-1Mo, (B) SS 316LN, (C) Macrograph of DMWJ, (D) Interface - P91-182B-1, (E) Interface - P91-182B-2, (F) 182 WM, (G) Interface-82/182 W-SS316LN.

The optical micrographs of different regions of DMWI are shown in Figure 7D-G and the macrograph of the joint is also included. The macrograph of DMWJ (Figure 7C) is free from cracks, and lack of fusion defects. The interface between Modified 9Cr-1Mo to Inconel 182 buttering is shown in Figure 7D which shows clear fusion boundary and tempered martensite structure in addition to that Type I (perpendicular to fusion boundary) and Type II (parallel to fusion boundary) boundaries are also visible. These Type I and Type II boundaries are formed during allotropic transformation (say from  $\delta$  to  $\gamma$ ) of the base metal that occurs on cooling and produces mobile grain boundaries of the  $\gamma/\gamma$  type at the fusion boundary in dissimilar metal (fcc/bcc) welds. It has been shown that type II boundaries can form in such dissimilar metal welds only when there is

a ferrite/austenite phase boundary at elevated temperature in the base metal. In the present work, the Inconel 182 weld metal solidifies in the austenitic mode in spite of the dilution from the base metal, while the modified 9Cr-1Mo base metal solidifies as ferrite and then undergoes transformations first to austenite and then to martensite [18]. Figure 7E shows the interface between modified 9Cr-1Mo to Inconel 182 buttering, the epitaxial solidification of austenite crystals is visible and it is oriented transverse to the welding direction. Since the filler metal consists of 70% nickel as an alloying element, the microstructure of Inconel 182 buttering is predominantly austenite with some secondary phase particles which is mainly of NbC identified in earlier studies [10]. The post heating of Inconel 182 buttering is having no effect on microstructure.

Figure 7F shows the optical micrograph of Inconel 82/182 weld metal which consists of solidification grain boundaries (SGB's) and migrated grain boundaries (MGB's). SGB's are the direct result of competitive growth that occurs along the trailing edge of the weld pool. The SGB that forms at the end of solidification has both a compositional and crystallographic component. In some situations, it is possible for the crystallographic component of the SGB to migrate away from the compositional component. This new boundary that carries with it the highangle misorientation of the "parent" SGB is called an MGB [19, 20]. Figure 7G shows the interface between Inconel 82/182 weld metal to 316LN HAZ which consists of an unmixed zone and coarse austenitic grains. The unmixed zone if formed due to total melting of SS 316LN base metal and resolidified without filler metal dilution and this zone is having the same composition of SS 316LN base metal.

# 4 Conclusions

The dissimilar joint between modified 9Cr-1Mo and SS316LN is successfully fabricated without any macro level defects. From this investigation, the following conclusions are derived.

- Transverse tensile properties of DMWJ is lower than the respective base metals and the failure occurs at the outer edge of the HAZ of modified 9Cr-1Mo ferritic steel side. The tensile strength of DMWJ is 39% lower than modified 9Cr-1Mo ferritic steel and 14% lower than 316LN austenitic stainless steel.
- Charpy V-notch impact toughness of DMWJ is lower than the base metals. The impact toughness is 84% lower than modified 9Cr-1Mo ferritic steel and 110% lower than 316LN austenitic stainless steel.
- The fracture surfaces of both tensile and impact specimens are dominated by ductile dimples with tear ridges which shows significant amount of plastic deformation is observed before final failure.
- A non-uniform microhardness profile was observed for DMWJ. A soft zone is formed around 4-5 mm from the interface between modified 9Cr-1Mo to Inconel 182 buttering. This result is consistent with transverse tensile properties of DMWJ.
- A complex microstructure was developed at the interface between modified 9Cr-1Mo to Inconel 182 buttering. The unmixed zone is also developed at the interface between Inconel 82/182 weld metal to SS316LN. These complex microstructures are developed due to the compositional mismatch between base and filler metals.

Acknowledgements: The authors are thankful to UGC-DAE consortium for providing financial assistance (Project No. CSR-KN/CRS-56/2013-14/655) to carry out this investigation. Authors are thankful to The Director, IGCAR, Kalpakkam for providing base metals to carry out this investigation. Authors wish to record their sincere thanks to M/s. Mailam India Pvt. Limited, Pondicherry for the consumables supply. Authors wish to express their gratitude to Dr. A. Moitra, Scientist-G, MMS/MTD for the help rendered in impact toughness testing.

#### References

- [1] Vitek JM, Klueh RL. Metall. Trans. A 1983, 14, 1047-1055.
- [2] Mathew MD. T. Indian I. Metals 2010, 63, 151-158.
- [3] Kumar P, Pai A. Procedia Eng. 2014, 86, 173-183.
- [4] Sireesha M, Albert SK, Shankar V, Sundaresan S. J. Nucl. Mater. 2000, 279, 65-76.
- [5] Zhang ZL, Hauge M, Thaulow C, Ødegård J. Eng. Fract. Mech. 2002, 69, 353-366.
- [6] Sireesha M, Albert SK, Sundaresan S. Int. J. Press. Ves. Pip. 2002, 79, 819-827.
- [7] Sireesha M, Albert SK, Sundaresan S. Metall. Mater. Trans. A 2005, 36, 10-12.
- [8] Lee HY, Lee SH, Kim JB, Lee JH. Int. J. Fatigue 2007, 29, 1868-1879.
- [9] Rathod DW, Pandey S, Singh PK, Prasad R. Mat. Sci. Eng. A 2015, 639, 259-268.
- [10] Falat L, Kepič J, Čiripová L, Ševc P, Dlouhý I. J. Mater. Res. 2016, 31, 1532-1543.
- [11] Rathod DW, Pandey S, Singh PK, Prasad R. J. Press. Vess. Technol. 2015, 138, 11403.
- [12] ASTM E8/E8M-16a, Standard Test Methods for Tension Testing of Metallic Materials, ASTM International, West Conshohocken, PA, 2016, www.astm.org.
- [13] ASTM E23-16b. Standard Test Methods for Notched Bar Impact Testing of Metallic Materials, ASTM International, West Conshohocken, PA, 2016, www.astm.org.
- [14] Laha K, Chandravathi KS, Parameswaran P, Rao KBS, Mannan SL. Metall. Mater. Trans. A 2007, 38, 58-68.
- [15] Viswanathan R, Henry JF, Tanzosh J, Stanko G, Shingledecker J, Vitalis B, Purgert R. J. Mater. Eng. Perform. 2005, 14, 281-292.
- [16] You YY, Shiue RK, Shiue RH, Chen C. J. Mater. Sci. Lett. 2001, 20, 1429-1432.
- [17] IGCAR, "PFBR/32040/SP/1002/R-0 Prototype Fast Breeder Reactor Specification for the Qualification of the Welding Consumables," Indira Gandhi Centre for Atomic Research, Kalpakkam, India, Report No. PFBR/32040/SP/1002/R-0.
- [18] Nelson TW, Lippold JC, Mills MJ. Sci. Technol. Weld. Joi. 1998, 3, 249-255.
- [19] Wang HT, Wang GZ, Xuan FZ, Tu ST. Fracture mechanism of a dissimilar metal welded joint in nuclear power plant. Eng. Fail. Anal. 2013, 28, 134-148.
- [20] Lippold JC. Welding Metallurgy and Weldability, Book, Wiley, 2014. Retrieved from https://books.google.co.in/ books?id=TFdVBOAAOBAI.